J Breast Cancer. 2019 Jun;22(2):155-171
https://doi.org/10.4048/jbc.2019.22.e26
pISSN 1738-6756·eISSN 2092-9900

Journal of Breast Cancer JBC

Review Article

Check for updates

Insights into Hypoxia: Non-invasive Assessment through Imaging Modalities and Its Application in Breast Cancer

Isaac Daimiel

Department of Radiology, Breast Imaging Service, Memorial Sloan Kettering Cancer Center, New York, NY, USA

OPEN ACCESS

Received: Jan 16, 2019
Accepted: Apr 15, 2019

Correspondence to
Isaac Daimiel
Department of Radiology, Breast Imaging Service, Memorial Sloan Kettering Cancer Center, 300 E 66th Street, New York, NY 10065, USA.
E-mail: idaimiel@hotmail.com

ORCID iDs
Isaac Daimiel
https://orcid.org/0000-0002-4878-1710

Funding
Isaac Daimiel was supported by a grant from the Spanish foundation "Fundación Alfonso Martín Escudero."

Conflict of Interest
The author has declared that they have no competing interests.

ABSTRACT

Oxygen is crucial to maintain the homeostasis in aerobic cells. Hypoxia is a condition in which cells are deprived of the oxygen supply necessary for their optimum performance. Whereas oxygen deprivation may occur in normal physiological processes, hypoxia is frequently associated with pathological conditions. It has been identified as a stressor in the tumor microenvironment, acting as a key mediator of cancer development. Numerous pathways are activated in hypoxic cells that affect cell signaling and gene regulation to promote the survival of these cells by stimulating angiogenesis, switching cellular metabolism, slowing their growth rate, and preventing apoptosis. The induction of dysregulated metabolism in cancer cells by hypoxia results in aggressive tumor phenotypes that are characterized by rapid progression, treatment resistance, and poor prognosis. A non-invasive assessment of hypoxia-induced metabolic and architectural changes in tumors is advisable to fully improve breast cancer (BC) patient management, by potentially reducing the need for invasive biopsy procedures and evaluating tumor response to treatment. This review provides a comprehensive overview of the molecular changes in breast tumors secondary to hypoxia and the non-invasive imaging alternatives to evaluate oxygen deprivation, with an emphasis on their application in BC and the advantages and limitations of the currently available techniques.

Keywords: Breast neoplasms; Hypoxia; Molecular imaging

INTRODUCTION

Hypoxia is defined as a lack of suitable oxygenation of cells, with low oxygen concentration within the tissues secondary to a discrepancy between oxygen supply and consumption. When this condition is physiological and usually transient, tissues are capable of regulating oxygen levels through vasodilation, reduction in oxygen consumption, and cellular triggering of alternative metabolic pathways. However, when the insult is long-lasting and homeostatic response mechanisms are not satisfactory, hypoxia becomes pathological. Thus, it is involved in the development and progression of certain diseases, such as cardiovascular disease, chronic kidney disease, and diabetic retinopathy, or inflammatory conditions like rheumatoid arthritis [1-5].

Several efforts to determine numerical cut-off values for hypoxia status have been made [6]. In breast tumors, partial pressure of oxygen (PaO_2) below 10 mmHg have been related to increased risk of mortality and metastasis [7]. Nevertheless, assigning cut-off values turns out to be challenging due to the presence of certain gaseous mediators such as nitric oxide. This is synthesized in a hypoxic environment to counteract the effects of the tissue oxygen deprivation changing the threshold, at which hypoxia might be considered pathological. Also, breast tissue has a complex architecture and a variable oxygen demand due to background physiological fluctuations secondary to menstrual cycle changes [8].

The study of hypoxia in oncology has implications in many types of cancers, including breast cancer (BC). It is crucial to understand the molecular mechanisms underlying hypoxia leading to tumor growth, so molecular imaging strategies can be developed, thus providing the oncology community with several options to choose from when assessing hypoxia.

Firstly, oxygen deprivation in breast tumors has implications for diagnosis and prognosis. Hypoxia is known as a key mediator process in cancer development and a tumor microenvironment stressor leading to dysregulated metabolism (metabolic switch). This results in aggressive tumor phenotypes that are characterized by increased risk of invasion and metastasis and a poor prognosis for survival and local control, independent of the clinical stage at diagnosis [9,10].

When tumors start to grow, there is a decreased delivery of oxygenated blood to meet the increased metabolic demands of the rapidly proliferating tumor cells. In response to the new situation, angiogenesis turns on through the activation of a sheer number of angiogenic factors such as interleukin-8, platelet derived growth factor, cyclooxygenase-2, endothelin-1 and -2, fibroblast growth factor-3, or nitric oxide synthase. Probably, members of the vascular endothelial growth factor (VEGF) family are the most relevant ones. These mediators trigger cellular responses by binding to membrane tyrosine kinase receptors, conforming dimers and becoming activated through transphosphorylation [11]. Overexpression of VEGF-A has been associated with decreased overall survival and disease-free survival in BC [12]. Likewise, this so called “angiogenic switch” has been implicated in tumor metastasis [13]. VEGF, in collaboration with other factors, is responsible for a network of microvasculature, which exhibit functional and structural abnormalities posing limitations to oxygen diffusion, and therefore aggravating tumor deprivation [14,15]. This forces the tumor cells to develop adaptive responses by changing gene expression that will contribute to their survival in a hostile hypoxic environment. A cornerstone in these adaptive responses is the hypoxia-inducible transcription factor (HIF) family [12].

HIF-1 is the best characterized member of the HIF family and plays a critical role in tumor adjustment to hypoxia. HIF-1 is a heterodimeric transcription factor consisting of an inducible α unit and a constitutively expressed β unit. When oxygen is present, HIF-1α is hydroxylated at several proline residues, leading to its ubiquitination and proteasomal degradation. However, under hypoxic conditions, HIF-1α evades degradation and assembles with HIF-1β, creating a transcription factor (HIF-1) that can bind to target genes in the nucleus through its 5′-TACGTG-3′ recognition sequence. Thus, there is an upregulation of genes involved in glucose metabolism, pH regulation, cellular proliferation and apoptosis, nitric oxide metabolism, intracellular reduction–oxidation homeostasis, angiogenesis, and erythropoiesis [16-22].

https://doi.org/10.4048/jbc.2019.22.e26

Although hypoxia is the most powerful stimulus for inducing HIFs, oxygen deprivation is not the only determinant of HIF production. Products of oncogenes, such as protein kinase B, can also activate HIFs. Likewise, the inhibition of tumor suppressors, such as phosphatase and tensin homolog, promyelocytic leukemia protein, or tuberous sclerosis complex, can stimulate the HIF response in normoxia, which increases the complexity of this molecular machinery [23] (**Figure 1**).

Secondly, hypoxia has implications for BC treatment. Notably, hypoxia can directly attenuate chemotherapeutic-agent action by reducing the generation of intracellular free radicals and, therefore, limiting the damage induced on DNA. It has been proposed as the mechanism of chemoresistance to agents used in BC treatment, such as anthracyclines [20,24]. The molecular changes mentioned, especially those that lead to genomic instability, extracellular acidification, resistance to apoptosis, evasion of immune system surveillance, and metastasis, seem to be deeply related to chemotherapy resistance [25].

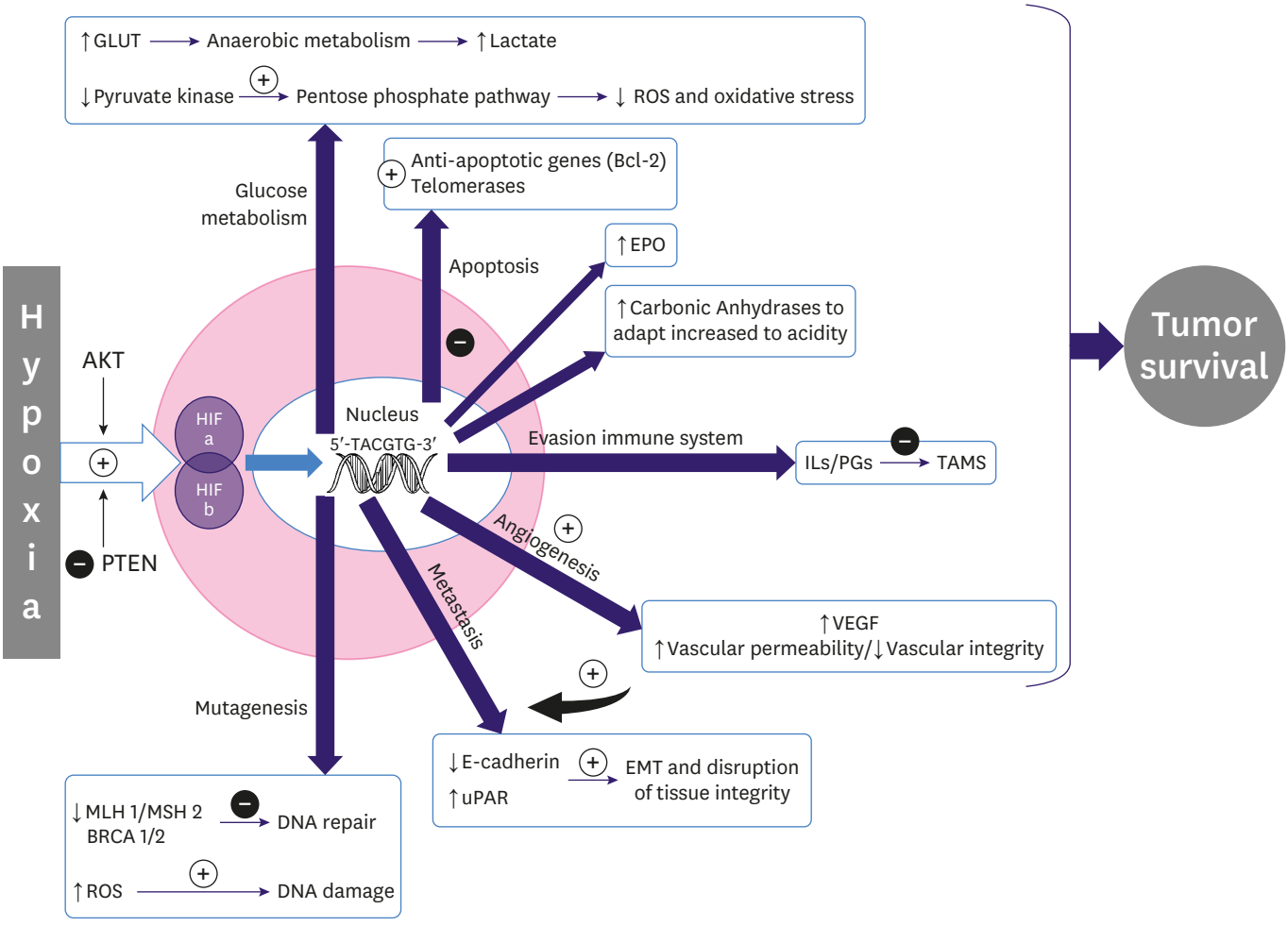

Figure 1. Diagram of the effects of hypoxia in tumor cells.
GLUT = glucose transporter; ROS = teactive oxygen species; Bcl-2 = B-cell lymphoma 2; EPO = erythropoietin; IL = interleukin; PG = prostaglandin; TAMS = tumor-associated macrophages; VEGF = vascular endotelial growth factor; uPAR = urokinase plasminogen activator receptor; HIF = hypoxia-inducible factor; BRCA 1/2 = breast cancer genes; PTEN = phosphatase and tensin homolog; AKT = protein kinase B; MSH 2 = mutS protein homolog 2; MLH 1 = mutL homolog 1.

https://doi.org/10.4048/jbc.2019.22.e26

One of the first reported molecular mechanisms explaining this contribution was the activation of the multidrug resistance 1 (*MDR1*) gene by HIF-1α in response to hypoxia. *MDR1* is responsible for the genesis of several membrane glycoproteins, finally clearing some chemotherapeutic drugs used in BC, such as vinca alkaloids, anthracyclines, and paclitaxel [26].

VEGF induced by HIF also helps to decrease functional concentrations of chemotherapeutic agents by inducing the formation of aberrant tumor blood vessels, which result in diminished and uneven distribution of the drugs. Increased glycolysis with extracellular acidosis may also affect the transport of drugs across the cell membrane, conditioning the therapeutic efficacy of a wide variety of agents used in BC, such as anthracyclines, cyclophosphamide, or carboplatin [24].

Recently, the importance of cancer stem cells (CSCs) and their contribution to therapeutic resistance and disease recurrence have been highlighted. These pluripotent cells within solid tumors have the ability of epithelial-mesenchymal transition, auto self-renewability, and drug resistibility. Hypoxia has been involved in the transformation and growth of these cellular pools [23,27]. The expansion of the CSC marker $CD133^+$ has been shown to be involved in the transition from in situ to invasive BC [21].

The deleterious role of hypoxia in radiotherapy is based on its own mechanism of action that is enhanced in the presence of oxygen. The radiation causes tissue damage through the formation of free radicals, directly on the target or indirectly through water tissue ionization. These free radicals will react rapidly with oxygen to become more stable, producing chemical changes in the composition of the cells and causing damage to DNA in the presence of oxygen. This is known as "oxygen enhancing effect." Conversely, under hypoxic conditions, the cell is unable to follow the sequence of reactions that prevent the tissue from being damaged, thus resulting in radiation resistance and local recurrence of the disease [28,29]. In addition, hypoxia may indirectly promote radioresistance through gene modification, decreasing apoptotic potential and diminishing proliferation, thereby reducing radiosensitivity of the tumor [20].

NON-INVASIVE IMAGING APPROACHES TO HYPOXIA

The ability to identify hypoxia would have implications in a wide range of oncological settings. On one hand, it would allow stratification of patients for more accurate prognostic information. On the other hand, identifying hypoxic tumors would improve patient outcomes by helping to adjust irradiation dose, selecting individuals for personalized treatment with anti-hypoxia-directed therapies, and finding new strategies to increase the efficacy of drugs by increasing oxygen supply to the tumor (e.g., the administration of recombinant human erythropoietin) [24,30].

To date, patient risk stratification and treatment decisions in BC are mainly based on the molecular profile of the tumor. Despite the importance of hypoxia, this parameter is not yet included in the decision-making flowchart in BC treatment. Non-invasive approaches for detecting and monitoring changes in tissue oxygenation will spearhead this change, since they are not conditioned by tumor location and can be repeated prior and during treatment, without causing any harm to the subject. Nevertheless, most non-invasive oximetry methods are not widely available in imaging centers and are still in a preclinical setting in need for

https://doi.org/10.4048/jbc.2019.22.e26

further research for validation. Positron emission tomography (PET) and blood oxygen level dependent magnetic resonance imaging (BOLD MRI) are the leading candidate methods for visualizing tissue hypoxia in human tumors.

The non-invasive imaging methods for oximetry can detect the presence of oxygen directly within the tissue or indirectly by the administration of tracers that accumulate or activate within the hypoxic cells or endogenous oxygen-dependent markers, such as hypoxia-related proteins [6,31] (**Table 1**).

RADIOISOTOPE TECHNIQUES

PET and single photon emission computed tomography (SPECT) rely on the detection of gamma ray photons. SPECT requires gamma-emitting radioisotopes, such as technetium-99m, while PET uses radiopharmaceuticals, usually labeled with fluorine-18 (^{18}F) or carbon-11. These molecules are generally delivered into the cells by the bloodstream. Emissions from the radioisotopes are detected by a gamma camera in SPECT, depicting areas with more blood supply and therefore more biological activity. PET images are obtained with scanners after radionuclides are incorporated into molecules used by the body (e.g., fludeoxyglucose as a glucose analogue), following positron–electron annihilation. Although SPECT images are easier to acquire, PET is the preferred method for imaging tumor hypoxia due to its high specificity and sensitivity to show physiological processes *in vivo* and better spatial resolution.

Nitroimidazoles are hypoxic selective compounds used as radiosensitizers and are now widely used for PET imaging of hypoxia. These substances are delivered to the cells through the blood supply and once inside, they follow a redox reaction by the action of xanthine oxidase. This process is reversible in normoxia; however, under hypoxic conditions, the reduced molecules cannot be oxidized again. These highly reactive reduced intermediates tend to bind to other macromolecules, permanently remaining trapped inside viable hypoxic cells and thus, permitting radioisotopic imaging of hypoxia [32].

^{18}F fluoromisoinidazole

^{18}F fluoromisoinidazole (^{18}F FMISO) is the PET tracer used most frequently to detect hypoxia with several studies conducted in BC [33-36]. ^{18}F FMISO-PET has a low resolution due to the tracer's slow pharmacokinetic profile. Its slow uptake and wash-out kinetics require approximately a 2 hours delay time between injection and imaging to permit clearance of ^{18}F FMISO from normoxic tissue that would potentially limit visual detection of hypoxic regions [29]. Despite these limitations, ^{18}F FMISO could be useful for planning intensity modulated radiation therapy [37].

^{18}F-fluoroazomycin arabinoside, ^{18}F-flortanidazole, and ^{18}F-labeled fluoroerythronitroimidazole

^{18}F-fluoroazomycin arabinoside (^{18}F FAZA) and ^{18}F-flortanidazole are more hydrophilic nitroimidazoles, improving imaging of tumor hypoxia contrast by a faster clearance from the blood and normal tissues [38].

^{18}F-labeled fluoroerythronitroimidazole has been used in mammary tumors in a preclinical setting, showing similar distribution features as ^{18}F FAZA [39].

https://doi.org/10.4048/jbc.2019.22.e26

Table 1. Non-invasive imaging methods to measure hypoxia

Technique	Reporter	Infomation of hypoxia	Mechanism	Advantages	Disadvantages
Radioisotope techniques					
PET	Tracers labeled with radioisotopes, usually ^{18}F, ^{11}C, ^{67}Cu	Indirectly/tissue	• Tracers are trapped in hypoxic cells and get accumulated • Images are formed from gamma-rays directly emitted from radionuclides in SPECT and after annihilation in PET	• Macroscopic scale assessment of the tumor • High sensitivity • Over time assessment of hypoxia	• Ionizing radiation • Perfusion dependant • Low spatial resolution • Short half-life radiotracers needed • Waste disposal • Less agents available than PET • Less spatial resolution
SPECT	Gamma-emitting radioisotopes				
Resonance techniques					
DCE MRI	Gadolinium based contrast agents	Indirectly/ intravascular-tissue	Contrast enhancement	• Over time assessment of hypoxia	• Perfusion dependent • Qualitative approach
BOLD MRI	deoxyHb as a endogenous marker	Directly/ intravascular	Difference in relaxivity of oxygenated and deoxygenated haemoglobin	• Short acquisition times • High spatial and temporal resolution • Hyperoxic gas challenge and over time hypoxia assessment • qBOLD quantitavive maps of pO_2	• Flow and perfusion dependant • Susceptible to motion artefacts • Voxel based measurements
TOLD MRI	Tissue water O_2 as a endogenous marker	Directly/tissue	Longitudinal relaxation of time of O_2 Tissue water	• Hyperoxic gas challenge and over time hypoxia assessment • Short adquisition times • Independent of perfusion	• Susceptible to motion artefacts • Throughput is quite modest
^{19}F MR oximetry	Fluorinate probes	Indirectly/tissue	Relaxation rate of fluorinate probes accumulated in macrophages in presence of oxygen	• Quantitative pO_2 measurements • High sensitivity • Correlates good with pO_2 • No tissue background signal • Response to hyperoxic challenges	• Susceptible to flow artefacts • Low availability • Dependent of the concentration of disolved O_2
MRS	Lactate as a endogenous marker	Directly/tissue	Different frequencies of resonation depending of molecular environment in a magnetic field	• Quantitative determination of hypoxia through metabolites	• Time consuming • Water signal suppression essential • Voxel dependent
EPR/ESR	Inyection of paramagnetic probe	Indirectly/tissue	Interaction of unpaired electrones of O_2 with paramagnetic probe and change in T_2 relaxation rate	• Quantitative assessment of pO_2 • Hyperoxic gas challenge and overtime assessment of hypoxia	• Lack of equipment • Probe concentration dependent
OMRI	Hyperpolarized probes for oximetry	Indirectly/tissue	Change of relaxivity due to reactive oxygen species with excitation of an exogenous radical	• High sensitivity also with low pO_2 concentrations	• High cost • Low resolution
Optical techniques					
Optical StO_2 measurements	Use of visible light and the special properties of photons to obtain images	Direct/intravascular and tissue	Optical absortion contrast between O_sHb and dHb	• Quantitative measurement of pO_2 • *In vivo*	• Perfusion dependent • Depht sensing limitation
Luminescence quenching	Luminescent probes	Direct/tissue	Dectection of quenching of intensity of luminescent probe in presence of oxygen by optical readout devices	• High spatial resolution • Quantitative measurement of pO_2 *in vivo* • Assessment of rapid changes in oxygenation status	• Low penetration of light
Cherenkov luminescence imaging	Phosphorescent probes for oxygen or hypoxia-activated molecules	Indirect/tissue	Cherenkov radiation	• Quantitative measurement of pO_2/hypoxia-activated molecules • *In vivo*	• Penetration of radiation

PET = positron emission tomography; ^{18}F = fluorine-18; ^{11}C = carbon-11; ^{67}Cu = copper-67; SPECT = single photon emission computed tomography; DCE = Dynamic contrast-enhanced; MRI = magnetic resonance imaging; BOLD = blood oxygen level dependent; deoxyHb = deoxyhemoglobin; qBOLD = quantitative blood oxygen level dependent; MRS = magnetic resonance spectroscopy; EPR = electron paramagnetic resonance; ESR = electron spin resonance; OMRI = Overhauser-enhanced magnetic resonance imaging.

https://doi.org/10.4048/jbc.2019.22.e26

^{18}F-labeled tracers favorably provide additional information regarding tumor status and response to treatment that targets hypoxia. So far, there is no agreement on which would be the best nitroimidazole tracer [6,29,40].

Thiosemicarbazones

Thiosemicarbazones belong to a chemically different group, labelled with a positron-emitting isotope of copper (Cu). Cu^{2+} is reduced to Cu^{1+} within the cytoplasm, and this reaction is reversible in the presence of oxygen. In this group, the specificity of hypoxia occurs when, under low oxygen conditions, the Cu^{1+} in the thiosemicarbazone complex cannot be converted to Cu^{2+} again. Then, following protonation, Cu^{1+} separates from the complex and is entrapped within the cells. They have high membrane permeability and fast uptake kinetics, which allow for rapid imaging after injection. Among its disadvantages, they exhibit cell-type specificity and reduced accumulation in mildly hypoxic tissues [6,41-43].

Though highly promising, radioisotope techniques do not directly provide PaO_2 values and should be performed in perfused tissues. Besides, the complexity of measurements, the low spatial resolution, the exposure of patients to ionizing radiation, and the difficulty to obtain tracers make clinical translation challenging [33].

RESONANCE TECHNIQUES

Conventional contrast-enhanced MRI is the standard technique for the diagnosis of BC, with high sensitivity and specificity. However, this method is quite limited in its ability to characterize the complex biology of breast tumors [44]. Dynamic contrast-enhanced (DCE) MRI has been suggested as useful for detecting tumor hypoxia [45,46]. MRI signals are produced through the administration of a bolus of gadolinium-based contrast agent after its distribution within the tissue. This provides information on perfusion and permeability with several limitations, since perfusion is not the only feature influencing PaO_2; thus, the estimates may not be accurate [29].

To overcome the limitations of DCE MRI when assessing hypoxia, this technique can be combined with other oximetric methods such as BOLD MRI, ^{19}F-oximetry, and magnetic resonance (MR) spectroscopy (MRS) [6].

Blood oxygen level dependent and tissue oxygen level dependent

MRI relies on a large external magnetic field and coils to detect the relaxation of atoms with magnetic moments, after the delivery of radiofrequency pulses. BOLD MRI uses the paramagnetic properties of deoxyhemoglobin (deoxyHb), exploiting the difference in relaxivity of oxygenated and deoxygenated hemoglobin to generate a signal. Although hydrogen-1 (^{1}H) MRI cannot directly visualize molecular oxygen, the paramagnetic properties of deoxyHb allow an inference of molecular oxygen by its relaxation time (changes in longitudinal relaxation time T_1 and transverse relaxation T_2^*).

BOLD MRI signals are related to vascular oxygenation and may allow direct estimates of PaO_2. The presence of deoxyHb in blood vessels causes a decrease in T_2^*, leading to darkening in tissues containing the vessel in a T_2^*-weighted imaging protocol. BOLD MRI has the advantage of both high spatial and temporal resolution and can detect spontaneous oxygen fluctuations, permitting the study of different areas of functional vasculature within a tumor [29,47].

https://doi.org/10.4048/jbc.2019.22.e26

Among its disadvantages, measurements can only be determined within a measured voxel that can include blood vessels and surrounding tissue, which in tumors is likely to contain tortuous microcapillaries, making BOLD MRI interpretation harder. A second limitation of BOLD MRI is that it reflects vascular oxygenation, which may be unrelated to tissue PaO_2, because of wall permeability and flow and oxygen content in the blood [48].

The use of BOLD MRI, in combination with other approaches derived from ^1H relaxation, may be able to overcome blood volume and flow limitations. These techniques are flow- and oxygen level-dependent in contrast to tissue oxygen level dependent (TOLD)/oxygen-enhanced MRI, which yields information on tissue PaO_2 [49]. Combining BOLD and TOLD MRI could provide a robust insight into tumor hypoxia [50,51]. TOLD MRI is a widely available method that uses a T_1-weighted protocol. It does not need any contrast agent and has short acquisition times that allow the monitoring of PaO_2 changes. TOLD MRI relies on oxygen as an endogenous contrast agent, using its paramagnetic properties that shorten T_1 of the surrounding protons, establishing a correlation between PaO_2 and relaxation rates. However, this correlation can be difficult to establish since T_1 is influenced by temperature, tumor features, and basal blood oxygen saturation [52,53].

Artifacts may represent another limitation for these techniques based on ^1H relaxation contrast. BOLD MRI is highly susceptible to motion artefacts. Specifically, the contrast of the image of the breast tissue in high fields can be affected by field distortions due to the complex breast geometry [54]. To improve signal contrast, protocols with $T2^*$-weighted fast spin echo images, rather than T_2^*-weighted gradient-recalled echo imaging, has been proposed [55].

BOLD MRI only provides qualitative or semi-quantitative information on PaO_2. A newly developed technique known as multiparametric quantitative BOLD (qBOLD) has achieved quantitative mapping of tumor hypoxia. It combines the possibility of monitoring changes in tumor oxygenation [48]. In breasts, several studies correlating relaxation rate $R2^*$ values with tumoral phenotype and HIF have been conducted, highlighting BOLD MRI as a useful tool with encouraging results [56,57].

MR oximetry based on perfluorocarbon [^{19}F MR]

The use of F-labeled contrast agents represents an alternate imaging approach to proton ^1H MRI, for depicting hypoxia. It allows us to map tumor hypoxia quantitatively and responds to hyperoxic challenges by displaying heterogeneity within each tumor [58,59].

^{19}F MR oximetry uses T_1 of fluorine agents, with the advantage of absolute determination of oxygenation *in vivo*. Also, acquisition times are short with few background signals.

Although promising, fluorine MR is expensive and the toxicity of perfluorocarbons (PFCs) chosen must be considered. PFCs like (^{19}F)-hexafluorobenzene also depend on the concentration of dissolved oxygen to be able to accumulate inside macrophages [60,61]. The way in which the fluorinated compounds reflect the oxygenation of different compartments requires additional investigation [29].

In addition to its use for evaluating hypoxia, ^{19}F MRI has been used in breast tumors to target cancer cells with nanoparticles for diagnosis or to assess the burden of tumor-associated macrophages within a tumor, to evaluate cancer progression and metastatic spread [62,63].

https://doi.org/10.4048/jbc.2019.22.e26

Also, images through F-labeled agents have demonstrated the ability to represent the oxygenation status according to hormonal levels [64].

MR spectroscopy

MRS exploits the nuclear spin properties of ^{1}H in a magnetic field, to absorb and emit radiofrequency. This technique obtains a spectrum of the concentration of metabolites resonating at different frequencies when placed in a magnetic field, because of their immediate molecular environment. Water signal suppression is essential for MRS image acquisition because the water proton signal is much stronger, due to its high concentration. Some products derived from hypoxia, such as lactate, can be determined with MRS imaging [43]. However, the study of hypoxia with MRS is time consuming and requires special analysis software.

Other atoms with unpaired protons, such as ^{31}P and ^{23}Na, have similar spin properties as ^{1}H. They can emit spatially localized signals in a spectrum. ^{31}P and ^{23}Na spectroscopic imaging and the determination of choline can be used for BC diagnosis, to increase specificity and monitor chemotherapy [44,65].

Electron paramagnetic resonance or electron spin resonance

This MR technique provides a quantitative assessment of the PaO_2 in the tissue. The principle of electron paramagnetic resonance (EPR) oximetry is that oxygen undergoes spin exchange interaction with paramagnetic species (molecules presenting unpaired electrons). EPR oximetry requires the injection of a paramagnetic probe into the tumors; thus, the unpaired oxygen electrons interact with the paramagnetic probe and cause a change in T_2^*. This can be observed by a change in the linewidth of the spectrum, with an increase in line-broadening of peak to peak widths, which can be used to infer oxygen concentration [66].

Measurements are non-invasive and dynamic oximetry and it is possible to show regional response of the tumor to hyperoxic gas challenge, reflecting differences in PaO_2 within the tumor [67]. The probe concentration and the fast relaxation of paramagnetic species can condition the evaluation. Coils enabling EPR imaging and MRI have been developed to correlate the PaO_2 maps with anatomical information and perfusion measurements [68].

For improving the sensitivity of this technique, a combined EPR/MR approach, Overhauser-enhanced MRI (OMRI) has been developed. This uses a low-field MR scanner and a paramagnetic contrast agent. The method exploits the Overhauser enhancement in the tissue water protons that is generated when a paramagnetic agent is hyperpolarized through electromagnetic irradiation; then, a transfer of electron polarization occurs toward the surrounding water's protons. Tumor perfusion and oxygenation can be analyzed using probes for oximetry like Oxo63. Image contrast is proportional to agent concentration in tumor perfusion, while it is inversely proportional to oxygen concentration [29].

Two types of paramagnetic materials can be used as probes: soluble materials (e.g., nitroxides and triaryl methyl radicals) and insoluble particulate materials (e.g., coals, chars, and inks). Insoluble agents have higher sensitivities for oxygen [69].

Although EPR oximetry is a promising technique for monitoring treatment through hypoxia, it is not yet utilized in BC, probably due to lack of sufficient development and adequate instrumentation.

https://doi.org/10.4048/jbc.2019.22.e26

OPTICAL IMAGING FOR MEASURING HYPOXIA

Some of the optical imaging methods to evaluate hypoxia, such as those used in histology, are invasive. They need tumor specimens to detect targeted hypoxia-inducible factors, such as HIF-1 or VEGF [67]. These endogenous biomarkers are frequently used to test the validity of other biomarkers of hypoxia.

A non-invasive optical approach to quantitatively determine the activity of hypoxia genes is by introducing transgenes with hypoxic response elements as promoter sequences coupled to reporter genes, which produce *in vivo* bioluminescent imaging such as luciferase or green fluorescent protein [70-72]. These imaging tools are useful for studying the biology of hypoxia and mechanisms of response to experimental therapy *in vivo* but are unlikely to have a role in humans.

Other optical imaging methods looking inside the body rely on the use of visible light and the special properties of photons to obtain detailed images of tissues and smaller structures, including cells and molecules. As light is used, ionizing radiation is not involved in generating images, and many different properties of a tissue can be measured at the same time with various colors of light.

Most of these optical techniques can measure oxygen in tissues using the absorption contrast from hemoglobin–oxygen binding and luminescence quenching by oxygen.

Absorption contrast imaging methods are based on the property of oxyhemoglobin and deoxyHb to absorb light across a different spectral range; thus, it is possible to calculate oxygen saturation. Several techniques have been developed using this physical property [69].

Pulse oximetry is probably the most familiar and the simplest one. It works by transmitting two wavelengths of light in which either one will be more absorbed by either oxyhemoglobin or deoxyHb. By measuring the differential absorption in the blood vessels, blood PaO_2 can be determined.

Diffuse optical spectroscopy and tomography (DOS/T) irradiate tissues with light of different wavelengths. Some photons are absorbed, whereas others are scattered. The latter ones can be redirected toward detectors generating attenuation spectra that can in turn generate three-dimensional tomograms of tissue parameters, including oxygen saturation, since light absorption can be measured at different distances and positions from the light source. DOS/T has been used in humans to determine breast density [73].

Also, imaging techniques based on optical contrast between oxyhemoglobin and deoxyHb can be combined with ultrasound detectors in a method called photoacoustic tomography. When a molecule absorbs light, the energy can be redistributed into the environment, creating a thermally induced pressure jump that emits detectable ultrasonic waves. This is called the photothermal effect. And it is why this technique overcomes the resolution limitations imposed by the two other methods—by being able to visualize the three-dimensional position of molecules in tissue [74]. Although its role in humans has not been evaluated, some early studies in intracranial tumors and placenta in animals show considerable promise [75,76] (**Figure 2**).

https://doi.org/10.4048/jbc.2019.22.e26

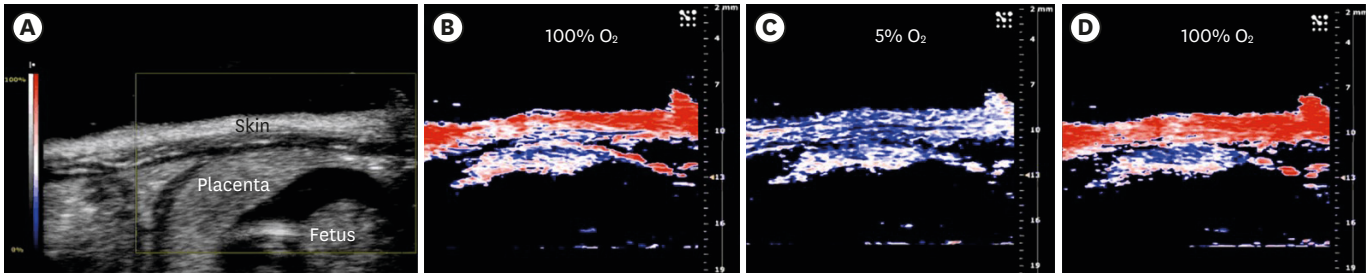

Figure 2. PA imaging of placental oxygenation on day 14 of gestation. (A) The placenta in a sagittal plane (obtained by a B-mode ultrasound scan) and parametric images created with the PA oxyhemo mode making possible the evaluation of blood oxygen saturation during variations in the oxygen levels supplied to the mother (5%–100%). PA imaging sequences during hyperoxygenation (B), hypoxia (C) and hyperoxygenation (D). Reprinted with permission from reference 76: Arthuis CJ, Novell A, Raes F, Escoffre JM, Lerondel S, et al. Real-time monitoring of placental oxygenation during maternal hypoxia and hyperoxygenation using photoacoustic imaging. PLoS One 2017;12:e0169850.
PA = photoacoustic.

Optical coherence tomography (OCT) is a noninvasive imaging technique that provides high resolution images of detailed structures of the tissues that are almost close to what histology may provide. OCT employs light from a broadband light source, creating cross-sectional images. It does this by measuring the echo time delay and intensity of the reflected and backscattered light, through the depth of the tissue along a point *in vivo* [77]. It has been used to detect skin and retinal cancer [78,79]. In breast, OCT has been demonstrated useful for the surgical margin assessment [80,81]. A newer OCT variant called spectral-domain OCT uses spectral detectors, allowing the inference of oxygen saturation through the absorption information encoded in the spectra [82].

Another technique in development is luminescence quenching, in which luminescent probes are used to report absolute oxygen concentration. These compounds transfer energy to nearby molecular oxygen and therefore no longer emit radiation. The oxygen-quenching effect is rapidly reversible, making this useful for observing rapid changes in oxygenation status, including reoxygenation. The search for newer luminescent probes will allow the assessment of hypoxia-induced factors, as well as a decrease in toxicity, providing new windows for hypoxia detection [68,83].

The demonstration of visible light emission during the radioactive decay of positron-emitting radionuclides represents a new method of molecular imaging called Cherenkov luminescence imaging. As PET radiotracers labeled with high-energy positron-emitters are used, some physical principles underlying this technique are shared with the ones in PET. The nucleus emits a high-energy positron, which, as a result of subsequent interactions with the tissue, loses its energy and decays, eventually producing a pair of photons (gamma rays) in a phenomenon known as annihilation. These photons will ultimately reach the detector of the PET scanner to generate an image.

The initial velocity of these positrons often momentarily exceeds the speed of light (in the tissue) satisfying the requirements for the production of Cherenkov radiation. This is produced when a charged particle travels with a velocity that exceeds the speed of light through an insulating medium, producing a local polarization along its way. When returning to equilibrium, Cherenkov radiation is emitted and thus can be detected by an optical imager equipped with a charged coupled device camera. Using selective probes for oxygen or hypoxia-activated molecules, Cherenkov luminescence imaging may represent an invaluable technique to measure hypoxia *in vivo* and monitor tumor response to hypoxia-targeted drugs [84,85] (**Figure 3**).

https://doi.org/10.4048/jbc.2019.22.e26

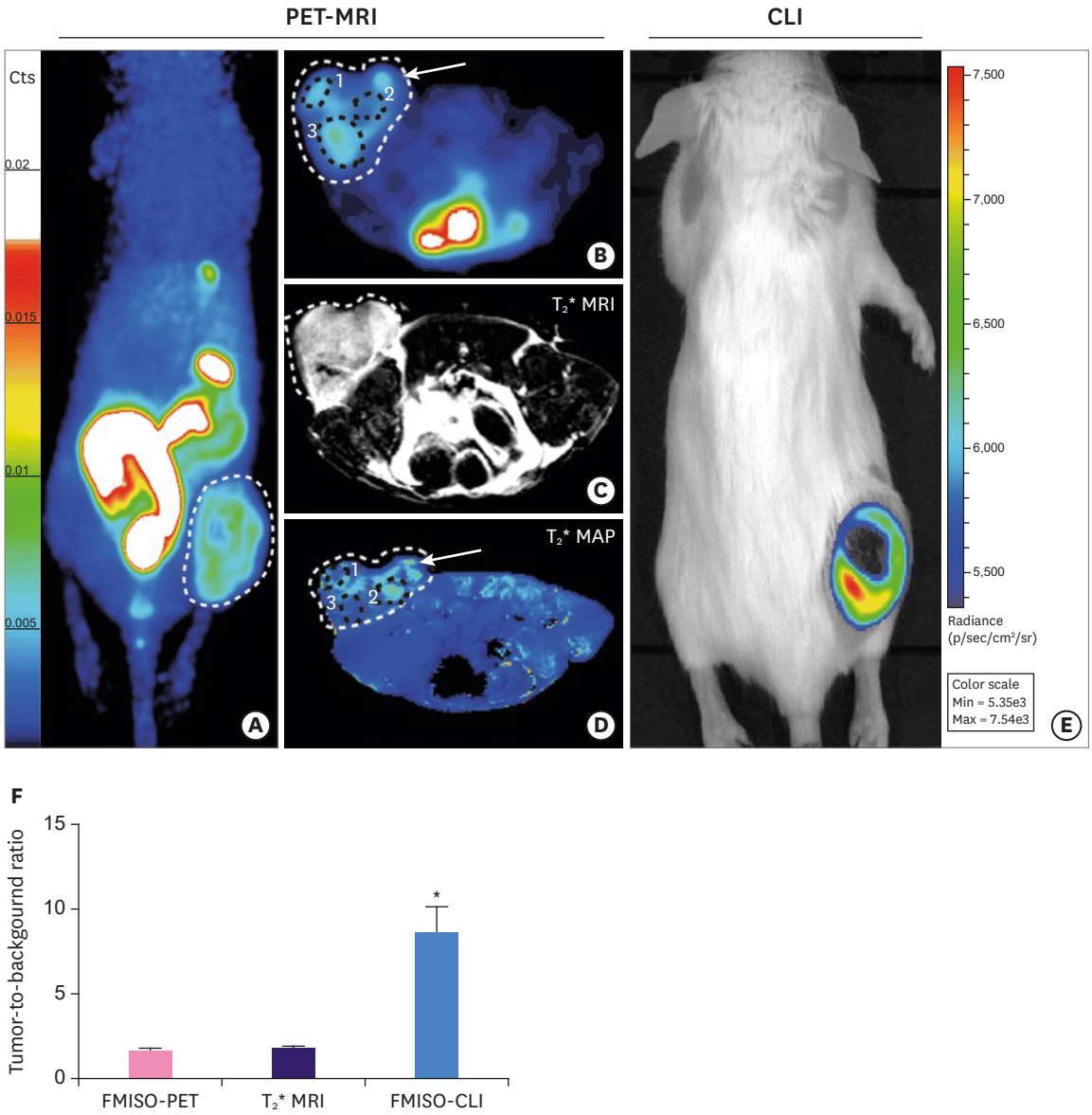

Figure 3. Imaging of hypoxia within CT26 tumour bearing mice (n = 13), PET-MRI: (A-D) Representative PET-MRI images showing the global co-localisation of FMISO uptake and BOLD MRI signal. Images were acquired 120 minutes post-injection of 10 MBq of ^{18}F FMISO PET. (A) Representative maximum-intensity-projection FMISO PET Image; (B) Transversal slice showing FMISO uptake within the tumour; (C) T_2^*-weighted MRI and (D) BOLD image derived from T_2^* mapping. White dashed lines: tumour limits, white arrows: oxygenated tumour area (increased BOLD signal), black circle: hypoxic tumour areas (decreased BOLD signal). CLI: (E) Representative FMISO CLI image of the same mouse as for (A) to (D) acquired just after the PET-MRI scan. (F) Tumour-to-background ratio for PET, MRI and CLI following the injection of FMISO determined by the ratio of the signal from the tumour and a contralateral irrelevant region of interest (muscle). Reprinted with permission from reference 85: Desvaux E, Courteau A, Bellaye P-S, Guillemin M, Drouet C, Walker P, et al. Cherenkov luminescence imaging is a fast and relevant preclinical tool to assess tumour hypoxia *in vivo*. EJNMMI Res 2018;8:111.
PET = positron emission tomography; MRI = magnetic resonance imaging; FMISO = fluoromisoinidazole; BOLD = blood oxygen level dependent; CLI = Cherenkov luminescence imaging.
*$p < 0.001$.

CONCLUSION

There is increasing evidence of the impact of hypoxia as a key inducer of metabolic and architectural changes within the tumor, which makes it more aggressive and resistant to drugs. The ability to non-invasively assess tumor oxygenation opens a new window to characterize the molecular profile of BC, to determine patient prognosis and personalize

https://doi.org/10.4048/jbc.2019.22.e26

treatments as well as evaluate tumor response to treatment. Further development of techniques to measure hypoxia within tissues will allow new breakthroughs in BC treatment.

ACKNOWLEDGMENTS

I would like to express my deepest appreciations to Simon Bailey MSci for the physics background.

REFERENCES

1. Hultén LM, Levin M. The role of hypoxia in atherosclerosis. Curr Opin Lipidol 2009;20:409-14.
PUBMED | CROSSREF
2. Taylor PC, Sivakumar B. Hypoxia and angiogenesis in rheumatoid arthritis. Curr Opin Rheumatol 2005;17:293-8.
PUBMED | CROSSREF
3. Ishida S, Shinoda K, Kawashima S, Oguchi Y, Okada Y, Ikeda E. Coexpression of VEGF receptors VEGF-R2 and neuropilin-1 in proliferative diabetic retinopathy. Invest Ophthalmol Vis Sci 2000;41:1649-56.
PUBMED
4. Mateo J, Izquierdo-Garcia D, Badimon JJ, Fayad ZA, Fuster V. Noninvasive assessment of hypoxia in rabbit advanced atherosclerosis using ^{18}f-fluoromisonidazole PET imaging. Circ Cardiovasc Imaging 2014;7:312-20.
PUBMED | CROSSREF
5. Fu Q, Colgan SP, Shelley CS. Hypoxia: the force that drives chronic kidney disease. Clin Med Res 2016;14:15-39.
PUBMED | CROSSREF
6. Bonnitcha P, Grieve S, Figtree G. Clinical imaging of hypoxia: current status and future directions. Free Radic Biol Med 2018;126:296-312.
PUBMED | CROSSREF
7. Vaupel P, Mayer A, Höckel M. Tumor hypoxia and malignant progression. Methods Enzymol 2004;381:335-54.
PUBMED | CROSSREF
8. Wallace TE, Patterson AJ, Abeyakoon O, Bedair R, Manavaki R, McLean MA, et al. Detecting gas-induced vasomotor changes via blood oxygenation level-dependent contrast in healthy breast parenchyma and breast carcinoma. J Magn Reson Imaging 2016;44:335-45.
PUBMED | CROSSREF
9. Vaupel P. Prognostic potential of the pre-therapeutic tumor oxygenation status. Adv Exp Med Biol 2009;645:241-6.
PUBMED | CROSSREF
10. Gilkes DM. Implications of hypoxia in breast cancer metastasis to bone. Int J Mol Sci 2016;17:E1669.
PUBMED | CROSSREF
11. Olsson AK, Dimberg A, Kreuger J, Claesson-Welsh L. VEGF receptor signalling - in control of vascular function. Nat Rev Mol Cell Biol 2006;7:359-71.
PUBMED | CROSSREF
12. Lu H, Shu XO, Cui Y, Kataoka N, Wen W, Cai Q, et al. Association of genetic polymorphisms in the VEGF gene with breast cancer survival. Cancer Res 2005;65:5015-9.
PUBMED | CROSSREF
13. Folkman J. Role of angiogenesis in tumor growth and metastasis. Semin Oncol 2002;29:15-8.
PUBMED | CROSSREF
14. Harris AL. Hypoxia--a key regulatory factor in tumour growth. Nat Rev Cancer 2002;2:38-47.
PUBMED | CROSSREF
15. Vaupel P, Harrison L. Tumor hypoxia: causative factors, compensatory mechanisms, and cellular response. Oncologist 2004;9 Suppl 5:4-9.
PUBMED | CROSSREF
16. Bristow RG, Hill RP. Hypoxia and metabolism. Hypoxia, DNA repair and genetic instability. Nat Rev Cancer 2008;8:180-92.
PUBMED | CROSSREF

17. Shaw RJ. Glucose metabolism and cancer. Curr Opin Cell Biol 2006;18:598-608.
PUBMED | CROSSREF

18. Dang CV, Semenza GL. Oncogenic alterations of metabolism. Trends Biochem Sci 1999;24:68-72.
PUBMED | CROSSREF

19. Semenza GL. Hydroxylation of HIF-1: oxygen sensing at the molecular level. Physiology (Bethesda) 2004;19:176-82.
PUBMED | CROSSREF

20. Adamaki M, Georgountzou A, Moschovi M. Cancer and the cellular response to hypoxia. Pediatr Therapeut 2012;S1:002.
PUBMED | CROSSREF

21. Gatenby RA, Smallbone K, Maini PK, Rose F, Averill J, Nagle RB, et al. Cellular adaptations to hypoxia and acidosis during somatic evolution of breast cancer. Br J Cancer 2007;97:646-53.
PUBMED | CROSSREF

22. Leek RD, Talks KL, Pezzella F, Turley H, Campo L, Brown NS, et al. Relation of hypoxia-inducible factor-2 alpha (HIF-2 alpha) expression in tumor-infiltrative macrophages to tumor angiogenesis and the oxidative thymidine phosphorylase pathway in Human breast cancer. Cancer Res 2002;62:1326-9.
PUBMED

23. Carnero A, Lleonart M. The hypoxic microenvironment: a determinant of cancer stem cell evolution. BioEssays 2016;38 Suppl 1:S65-74.
PUBMED | CROSSREF

24. Harrison L, Blackwell K. Hypoxia and anemia: factors in decreased sensitivity to radiation therapy and chemotherapy? Oncologist 2004;9 Suppl 5:31-40.
PUBMED | CROSSREF

25. Terry S, Faouzi Zaarour R, Hassan Venkatesh G, Francis A, El-Sayed W, Buart S, et al. Role of hypoxic stress in regulating tumor immunogenicity, resistance and plasticity. Int J Mol Sci 2018;19:E3044.
PUBMED | CROSSREF

26. Nardinocchi L, Puca R, Sacchi A, D'Orazi G. Inhibition of HIF-1alpha activity by homeodomain-interacting protein kinase-2 correlates with sensitization of chemoresistant cells to undergo apoptosis. Mol Cancer 2009;8:1.
PUBMED | CROSSREF

27. De Francesco EM, Maggiolini M, Tanowitz HB, Sotgia F, Lisanti MP. Targeting hypoxic cancer stem cells (CSCs) with Doxycycline: implications for optimizing anti-angiogenic therapy. Oncotarget 2017;8:56126-42.
PUBMED | CROSSREF

28. Gray LH, Conger AD, Ebert M, Hornsey S, Scott OC. The concentration of oxygen dissolved in tissues at the time of irradiation as a factor in radiotherapy. Br J Radiol 1953;26:638-48.
PUBMED | CROSSREF

29. Colliez F, Gallez B, Jordan BF. Assessing tumor oxygenation for predicting outcome in radiation oncology: a review of studies correlating tumor hypoxic status and outcome in the preclinical and clinical settings. Front Oncol 2017;7:10.
PUBMED | CROSSREF

30. Overgaard J. Hypoxic radiosensitization: adored and ignored. J Clin Oncol 2007;25:4066-74.
PUBMED | CROSSREF

31. Vordermark D, Horsman MR. Hypoxia as a biomarker and for personalized radiation oncology. Recent Results Cancer Res 2016;198:123-42.
PUBMED | CROSSREF

32. Wardman P. Chemical radiosensitizers for use in radiotherapy. Clin Oncol (R Coll Radiol) 2007;19:397-417.
PUBMED | CROSSREF

33. Fleming IN, Manavaki R, Blower PJ, West C, Williams KJ, Harris AL, et al. Imaging tumour hypoxia with positron emission tomography. Br J Cancer 2015;112:238-50.
PUBMED | CROSSREF

34. Ueda S, Saeki T, Osaki A, Yamane T, Kuji I. Bevacizumab induces acute hypoxia and cancer progression in patients with refractory breast cancer: multimodal functional imaging and multiplex cytokine analysis. Clin Cancer Res 2017;23:5769-78.
PUBMED | CROSSREF

35. Quintela-Fandino M, Lluch A, Manso L, Calvo I, Cortes J, García-Saenz JA, et al. ^{18}F-fluoromisonidazole PET and activity of neoadjuvant nintedanib in early HER2-negative breast cancer: a window-of-opportunity randomized trial. Clin Cancer Res 2017;23:1432-41.
PUBMED | CROSSREF

36. Cheng J, Lei L, Xu J, Sun Y, Zhang Y, Wang X, et al. ^{18}F-fluoromisonidazole PET/CT: a potential tool for predicting primary endocrine therapy resistance in breast cancer. J Nucl Med 2013;54:333-40.
PUBMED | CROSSREF

37. Hypoxia-positron emission tomography (PET) and intensity modulated proton therapy (IMPT) dose painting in patients with chordomas. ClinicalTrials.gov Identifier: NCT00713037. 2017. U.S. National Library of Medicine. https://clinicaltrials.gov/ct2/show/NCT00713037. Accessed Month Day, Year.

38. Reischl G, Dorow DS, Cullinane C, Katsifis A, Roselt P, Binns D, et al. Imaging of tumor hypoxia with [124I]IAZA in comparison with [18F]FMISO and [18F]FAZA--first small animal PET results. J Pharm Pharm Sci 2007;10:203-11.
PUBMED

39. Grönroos T, Bentzen L, Marjamäki P, Murata R, Horsman MR, Keiding S, et al. Comparison of the biodistribution of two hypoxia markers [^{18}F]FETNIM and [^{18}F]FMISO in an experimental mammary carcinoma. Eur J Nucl Med Mol Imaging 2004;31:513-20.
PUBMED | CROSSREF

40. Xu Z, Li XF, Zou H, Sun X, Shen B. ^{18}F-Fluoromisonidazole in tumor hypoxia imaging. Oncotarget 2017;8:94969-79.
PUBMED

41. Vāvere AL, Lewis JS. Cu-ATSM: a radiopharmaceutical for the PET imaging of hypoxia. Dalton Trans 2007;(43):4893-902.
PUBMED | CROSSREF

42. Horsman MR, Mortensen LS, Petersen JB, Busk M, Overgaard J. Imaging hypoxia to improve radiotherapy outcome. Nat Rev Clin Oncol 2012;9:674-87.
PUBMED | CROSSREF

43. Challapalli A, Carroll L, Aboagye EO. Molecular mechanisms of hypoxia in cancer. Clin Transl Imaging 2017;5:225-53.
PUBMED | CROSSREF

44. Pinker K, Helbich TH, Morris EA. The potential of multiparametric MRI of the breast. Br J Radiol 2017;90:20160715.
PUBMED | CROSSREF

45. Jensen RL, Mumert ML, Gillespie DL, Kinney AY, Schabel MC, Salzman KL. Preoperative dynamic contrast-enhanced MRI correlates with molecular markers of hypoxia and vascularity in specific areas of intratumoral microenvironment and is predictive of patient outcome. Neuro-oncol 2014;16:280-91.
PUBMED | CROSSREF

46. Halle C, Andersen E, Lando M, Aarnes EK, Hasvold G, Holden M, et al. Hypoxia-induced gene expression in chemoradioresistant cervical cancer revealed by dynamic contrast-enhanced MRI. Cancer Res 2012;72:5285-95.
PUBMED | CROSSREF

47. Baudelet C, Gallez B. How does blood oxygen level-dependent (BOLD) contrast correlate with oxygen partial pressure (pO_2) inside tumors? Magn Reson Med 2002;48:980-6.
PUBMED | CROSSREF

48. Christen T, Lemasson B, Pannetier N, Farion R, Remy C, Zaharchuk G, et al. Is T2* enough to assess oxygenation? Quantitative blood oxygen level-dependent analysis in brain tumor. Radiology 2012;262:495-502.
PUBMED | CROSSREF

49. Howe FA, Robinson SP, Rodrigues LM, Griffiths JR. Flow and oxygenation dependent (FLOOD) contrast MR imaging to monitor the response of rat tumors to carbogen breathing. Magn Reson Imaging 1999;17:1307-18.
PUBMED | CROSSREF

50. Mason RP, Zhao D, Pacheco-Torres J, Cui W, Kodibagkar VD, Gulaka PK, et al. Multimodality imaging of hypoxia in preclinical settings. Q J Nucl Med Mol Imaging 2010.54:259-80.
PUBMED

51. White DA, Zhang Z, Li L, Gerberich J, Stojadinovic S, Peschke P, et al. Developing oxygen-enhanced magnetic resonance imaging as a prognostic biomarker of radiation response. Cancer Lett 2016;380:69-77.
PUBMED | CROSSREF

52. Ding Y, Mason RP, McColl RW, Yuan Q, Hallac RR, Sims RD, et al. Simultaneous measurement of tissue oxygen level-dependent (TOLD) and blood oxygenation level-dependent (BOLD) effects in abdominal tissue oxygenation level studies. J Magn Reson Imaging 2013;38:1230-6.
PUBMED | CROSSREF

53. O'Connor JP, Robinson SP, Waterton JC. Imaging tumour hypoxia with oxygen-enhanced MRI and BOLD MRI. Br J Radiol 2019;92:20180642.
PUBMED | CROSSREF

54. Maril N, Collins CM, Greenman RL, Lenkinski RE. Strategies for shimming the breast. Magn Reson Med 2005;54:1139-45.
PUBMED | CROSSREF

55. Rakow-Penner R, Daniel B, Glover GH. Detecting blood oxygen level-dependent (BOLD) contrast in the breast. J Magn Reson Imaging 2010;32:120-9.
PUBMED | CROSSREF

56. Liu M, Guo X, Wang S, Jin M, Wang Y, Li J, et al. BOLD-MRI of breast invasive ductal carcinoma: correlation of R2* value and the expression of HIF-1α. Eur Radiol 2013;23:3221-7.
PUBMED | CROSSREF

57. Choi HY, Ko ES, Han BK, Kim EJ, Kim SM, Lim Y, et al. Prognostic significance of transverse relaxation rate (R2*) in blood oxygenation level-dependent magnetic resonance imaging in patients with invasive breast cancer. PLoS One 2016;11:e0158500.
PUBMED | CROSSREF

58. Hunjan S, Zhao D, Constantinescu A, Hahn EW, Antich PP, Mason RP. Tumor oximetry: demonstration of an enhanced dynamic mapping procedure using fluorine-19 echo planar magnetic resonance imaging in the Dunning prostate R3327-AT1 rat tumor. Int J Radiat Oncol Biol Phys 2001;49:1097-108.
PUBMED | CROSSREF

59. Zhao D, Jiang L, Hahn EW, Mason RP. Comparison of ^{1}H blood oxygen level-dependent (BOLD) and ^{19}F MRI to investigate tumor oxygenation. Magn Reson Med 2009;62:357-64.
PUBMED | CROSSREF

60. Le D, Mason RP, Hunjan S, Constantinescu A, Barker BR, Antich PP. Regional tumor oxygen dynamics: 19F PBSR EPI of hexafluorobenzene. Magn Reson Imaging 1997;15:971-81.
PUBMED | CROSSREF

61. Procissi D, Claus F, Burgman P, Koziorowski J, Chapman JD, Thakur SB, et al. *In vivo* ^{19}F magnetic resonance spectroscopy and chemical shift imaging of tri-fluoro-nitroimidazole as a potential hypoxia reporter in solid tumors. Clin Cancer Res 2007;13:3738-47.
PUBMED | CROSSREF

62. Zhang C, Moonshi SS, Wang W, Ta HT, Han Y, Han FY, et al. High F-content perfluoropolyether-based nanoparticles for targeted detection of breast cancer by ^{19}F magnetic resonance and optical imaging. ACS Nano 2018;12:9162-76.
PUBMED | CROSSREF

63. Makela AV, Foster PJ. Imaging macrophage distribution and density in mammary tumors and lung metastases using fluorine-19 MRI cell tracking. Magn Reson Med 2018;80:1138-47.
PUBMED | CROSSREF

64. Bartusik D, Tomanek B, Siluk D, Kaliszan R, Fallone G. The application of ^{19}F magnetic resonance *ex vivo* imaging of three-dimensional cultured breast cancer cells to study the effect of δ-tocopherol. Anal Biochem 2009;387:315-7.
PUBMED | CROSSREF

65. O'Flynn EA, DeSouza NM. Functional magnetic resonance: biomarkers of response in breast cancer. Breast Cancer Res 2011;13:204.
PUBMED | CROSSREF

66. Velan SS, Spencer RG, Zweier JL, Kuppusamy P. Electron paramagnetic resonance oxygen mapping (EPROM): direct visualization of oxygen concentration in tissue. Magn Reson Med 2000;43:804-9.
PUBMED | CROSSREF

67. Krohn KA, Link JM, Mason RP. Molecular imaging of hypoxia. J Nucl Med 2008;49 Suppl 2:129S-48S.
PUBMED | CROSSREF

68. Krishna MC, Matsumoto S, Yasui H, Saito K, Devasahayam N, Subramanian S, et al. Electron paramagnetic resonance imaging of tumor pO_2. Radiat Res 2012;177:376-86.
PUBMED | CROSSREF

69. Roussakis E, Li Z, Nichols AJ, Evans CL. Oxygen-sensing methods in biomedicine from the macroscale to the microscale. Angew Chem Int Ed Engl 2015;54:8340-62.
PUBMED | CROSSREF

70. Shibata T, Giaccia AJ, Brown JM. Development of a hypoxia-responsive vector for tumor-specific gene therapy. Gene Ther 2000;7:493-8.
PUBMED | CROSSREF

71. Vordermark D, Shibata T, Brown JM. Green fluorescent protein is a suitable reporter of tumor hypoxia despite an oxygen requirement for chromophore formation. Neoplasia 2001;3:527-34.
PUBMED | CROSSREF

72. Harada H, Kizaka-Kondoh S, Hiraoka M. Optical imaging of tumor hypoxia and evaluation of efficacy of a hypoxia-targeting drug in living animals. Mol Imaging 2005;4:182-93.
PUBMED | CROSSREF

73. Blackmore KM, Knight JA, Walter J, Lilge L. The association between breast tissue optical content and mammographic density in pre- and post-menopausal women. PLoS One 2015;10:e0115851.
PUBMED | CROSSREF

74. Wang LV, Hu S. Photoacoustic tomography: *in vivo* imaging from organelles to organs. Science 2012;335:1458-62.
PUBMED | CROSSREF

75. Lungu GF, Li ML, Xie X, Wang LV, Stoica G. *In vivo* imaging and characterization of hypoxia-induced neovascularization and tumor invasion. Int J Oncol 2007;30:45-54.
PUBMED

76. Arthuis CJ, Novell A, Raes F, Escoffre JM, Lerondel S, Le Pape A, et al. Real-time monitoring of placental oxygenation during maternal hypoxia and hyperoxygenation using photoacoustic imaging. PLoS One 2017;12:e0169850.
PUBMED | CROSSREF

77. Nam HS, Yoo H. Spectroscopic optical coherence tomography: a review of concepts and biomedical applications. Appl Spectrosc Rev 2018;53:91-111.
CROSSREF

78. Reddy N, Nguyen BT. The utility of optical coherence tomography for diagnosis of basal cell carcinoma: a quantitative review. Br J Dermatol 2019;180:475-83.
PUBMED | CROSSREF

79. Neupane R, Gaudana R, Boddu SH. Imaging techniques in the diagnosis and management of ocular tumors: prospects and challenges. AAPS J 2018;20:97.
PUBMED | CROSSREF

80. Ha R, Friedlander LC, Hibshoosh H, Hendon C, Feldman S, Ahn S, et al. Optical coherence tomography: a novel imaging method for post-lumpectomy breast margin assessment-a multi-reader study. Acad Radiol 2018;25:279-87.
PUBMED | CROSSREF

81. Singla N, Dubey K, Srivastava V. Automated assessment of breast cancer margin in optical coherence tomography images via pretrained convolutional neural network. J Biophotonics 2019;12:e201800255.
PUBMED | CROSSREF

82. Schuman JS. Spectral domain optical coherence tomography for glaucoma (an AOS thesis). Trans Am Ophthalmol Soc 2008;106:426-58.
PUBMED

83. Sandhu S, Kydd L, Jaworski J. Luminescent probe based techniques for hypoxia imaging. J Nanomed Res 2017;6:00160.
PUBMED

84. Ciarrocchi E, Belcari N. Cerenkov luminescence imaging: physics principles and potential applications in biomedical sciences. EJNMMI Phys 2017;4:14.
PUBMED

85. Desvaux E, Courteau A, Bellaye PS, Guillemin M, Drouet C, Walker P, et al. Cherenkov luminescence imaging is a fast and relevant preclinical tool to assess tumour hypoxia *in vivo*. EJNMMI Res 2018;8:111.
PUBMED | CROSSREF